Available online at www.sciencedirect.com

ScienceDirect

Procedia Engineering 167 (2016) 129 – 137

Procedia Engineering

www.elsevier.com/locate/procedia

Comitato Organizzatore del Convegno Internazionale DRaF 2016, c/o Dipartimento di Ing. Chimica, dei Materiali e della Prod.ne Ind.le

Numerical/Experimental Study Of The Impact and Compression After Impact On GFRP Composite For Wind/Marine Applications

G. Perillo[a]*, J. K. Jørgensen[b]

[a] *SINTEF Materials and Chemistry Department of Materials and Nanotechnology – Trondheim - Norway*
[b] *SINTEF Materials and Chemistry Department of Materials and Nanotechnology – Oslo - Norway*

Abstract

Damage development due to impact needs to be understood to evaluate the consequences of impact on composite structures. This study concentrates on modelling low velocity impact and consequent compression after impact (CAI) test on thick industrial composites made from glass fiber epoxy produced by vacuum assisted resin infusion. Cross-plied laminates were tested with different impact energies and different numbers of interfaces (clustering). Results were compared to a 3D finite element analysis. Interfaces and their damage development were modelled with cohesive elements. Intraply properties were modelled by progressive failure analysis. The results show that the numerical model using only simple and independently measured material data was able to predict the impact and CAI behavior for the different energies and different stacking sequences.

Peer-review under responsibility of the Organizing Committee of DRaF2016

Keywords: Composite, GFRP, Low velocity impact, CAI, Experimental, FEM

1. Introduction

Composite structures are extremely susceptible to impact damage [1]. The consequences of impact can results in a large reduction of the structural performance with the possibility of catastrophic failure. More importantly, the damage can easily propagate under cyclic loads, which for instance commonly occur in marine and wind turbine

* Corresponding author. Tel: +47 47160974
E-mail address: giovanni.perillo@sintef.no

Peer-review under responsibility of the Organizing Committee of DRaF2016
doi:10.1016/j.proeng.2016.11.679

applications, producing even larger reductions in stiffness and eventually unexpected structural failure under normal design load conditions [2].

Impact is a complex interaction of an object with a structural component. It typically induces matrix cracking, fibre failure and delamination [1] that can highly decrease the stiffness of the material. Impact events have for long been investigated for thin carbon laminates produced by autoclave processes and used for high tech applications [1]. On the other hand, very few studies have been presented about impact on thicker glass fibers laminates produced by vacuum infusion or hand layup, as common practice in the marine wind energy industry [3].

González [4] performed a broad study, comparing numerical results with experimental impact and compression after impact (CAI) tests. An advanced interface model, based on the work by Turon [5], was used to model delamination. The intralaminar effects were evaluated using the LaRC04 failure theory developed by Maimi [6-8]. An advanced and innovative approach was presented by Bouvet [9], where discrete interface elements were used to simulate both the interlaminar and intralaminar damages during the impact. The same approach was used by Rivallant [10] for modelling the CAI tests. All these methods gave good agreement between theory and experiments, but they need an extensive set of input parameters requiring large and complicated test programs.

The simulation of low velocity impact event and the subsequent CAI requires: 1) definition of the impact scenario, 2) simulation of the impact event and consequent induced damage 3) assessment of the residual stiffness by in plane compression evaluation (CAI). This paper present a complete methodology capable to easily simulate the impact damage and asses the residual strength by using a simple numerical methodology based on readily available material parameters common available also for "low cost" applications.

The developed numerical model, used for both the impact and the CAI simulation, is based on 3D finite element model using cohesive elements for the interlaminar damage and a strength based failure criterion (based on Puck [11, 12] and Hashin [13]) for the intralaminar damage. This approach is fairly complicated to model and requires long computation times, but it is available to most engineers. Numerical results are compared to experimental tests on simple flat, cross-plied laminates with different stacking sequences impacted with different energies.

This is seen as a step to build up confidence in the modelling methods, eventually allowing engineers to design impact resistance of low cost composites reducing experimental testing.

Table 1: Summary of the tested material properties for the used HiPer-Tex E-Glass fibre / Momentive EPIKOTE MGS 135 resin and EPIKURE MGS 137 composite produced by vacuum infusion

Ply properties:

Properties	Value
Ply Thickness	0.86 mm
Density	1230 kg/m^3
Elastic properties	E_1= 44.87 *GPa*; E_2= E_3*= 12.13 *GPa*; G_{12}=G_{13}*=G_{23}*=3.38 *GPa;* ν_{12}=ν_{13}*=0.30; ν_{23}*=0.5
Strength *[MPa]***	X_t=1006.30; X_c=487.00; Y_t=Z_t*=45.95; Y_c= Z_c*=131.90; S_{12}= S_{13}*= S_{23}*=49.51;

Interface properties:

Properties	Value
Elastic properties	K_{nn}*= 12.13 *GPa*; K_{ss}*= K_{tt}*= 3.38 *GPa*
Strength *[MPa]*	t_n*=45.95; t_s*= t_t*=49.51;
Fracture toughness *[N/mm]*	G_{Ic}=0.98; G_{IIc}= G_{IIIc}*=3.71
Mode interaction – BK	η=1.40

**Assumed*

***Note: X is the fibre direction, Y is the matrix direction, t is for tension and c for compression; S_{12} is for shear*

2. Experimental Test

2.1. Material, Layup and geometry

The experimental tests were performed on E-Glass epoxy composite produced by vacuum assisted resin infusion, as commonly used in wind turbines, ships and offshore applications. The chosen reinforcement was a Seartex unidirectional stitch bonded mat made from 3B´s HiPer-tex W2020 E-Glass fiber with an average weight of 1150 g/m^2. Momentive Epikote MGS 135 epoxy resin with Epikure MGS 137 curing agent was used as resin. A mix ratio of 100:30 was selected with a curing time of 24h at room temperature and post curing at 80°C degrees for 15 hours.

As initial part of the work, the material properties were fully characterized. Unidirectional ply properties were measured for this material and results are summarized in Table 1 [14]. The Table also shows some assumed through

thickness ply properties that are cannot be measured with the traditional and standardized test methods. The values were chosen based on symmetry considerations for orthotropic plies.

Three different cross plied laminates were tested. All laminates had eight plies and a thickness of 6.8 ± 0.2 mm. The laminates are referred here as L1 $[0,0,90,90]_s$, L2 $[0,90,90,0]_s$ and L3 $[0,90,0,90]_s$. The three laminates have the same in plane laminate properties due to the same amount of plies in 0 and 90 directions. The important difference between the laminates is the number of interfaces (nd) where delamination can propagate (L1 nd=2, L2 nd=4 and L3 nd=6) due to the different plies clustering. For this reason delamination shape and dimensions are expected to vary for each laminate (for the same impact energy). The different layups were selected for evaluating the accuracy of the developed numerical method increasing the complexity of the model.

2.2. Drop weight test

The impact tests were performed according to the standard test method ASTM D7136 [15] in an Instron CEAST 9350 drop tower machine equipped with a high speed data acquisition system CEAST DAS 64K. A cylindrical impactor of 5.02 kg with 20 mm diameter spherical end was used.

According to the ASTM D7136 [15] standard, the test specimens had the dimensions 150±0.1 x 100±0.1 mm. They were supported on all sides in such a way that only a central region of 125 x 75 mm was free to deform under the impact. A special clamping system was adopted to prevent out-of-plane movements of the sample during the impact event. Details about the test configuration are shown in Figure 1. The impact force was measured by an accelerometer embedded in the impactor head via a high-speed data acquisition system triggered on the impact. An acquisition frequency of 1,000 kHz was used for all the tests.

The samples were tested with different impact energies. The test standard ASTM D7136 [15] suggests an impact energy of 45.5J (velocity of 4.25 m/s) for the given specimen thickness. All laminates were tested with this energy. Two other energies were also used for the laminate L2: 22.70 J (velocity of 3.00 m/s) and 68.25 J (velocity of 5.2 m/s), which represent +50% and -50% of the reference energy. Six samples were tested for each combination of layup and energy for a total of thirty impact tests: L1 (45.5J) - L2 (22.70J, 45.5J and 68.25J) – L3 (45.5J).

Figure 1: Drop weight test and CAI test

2.3. Compression after impact test

The Compression After Impact CAI test was performed on each of the impacted samples, following the recommendations of ASTM standard D7137 [16]. Five of the six impacted samples for each layup and impact energy were tested to evaluate their residual strength. Moreover, seven samples for layup 2 with no impact damage were also tested to evaluate the reference compressive strength of the undamaged material.

All tests were conducted in displacement control using a Schenck 250 kN servo hydraulic test machine. The compressive displacement was applied at a constant rate of 0.25 mm/min to avoid any inertial effects induced by high strain rate. In addition, due to the translucent nature of the E-Glass/Epoxy used in this work, the damage

development induced by the load application was monitored and recorded using the backlight technique and a high-speed camera.

3. Numerical methodology

3.1. Intralaminar damage model

Matrix cracking was evaluated by the Puck criterion [11] and fibre failure by the Hashin criteria [13]. Both methods were applied on the ply level using a user defined material model coded in a VUMAT subroutine, written in FORTRAN, for Abaqus/Explicit [17]. Ply damage was evaluated in each integration point at every step of the simulation. The Puck criterion is well suited for modelling impact due to its capability to consider also the out of plane components of the stresses in the failure evaluation. The detailed description of Hashin and Puck criteria is not reported here and can be found in the following publication [18, 19].

3.2. Interlaminar damage model

Delamination onset and propagation was modelled by the use of a cohesive zone model (CZM). The classical energy based bi-linear traction-separation law was used in the cohesive zone elements. The cohesive behaviour was defined directly in terms of a traction-separation law based on the following assumptions:

- Linear elastic traction-separation law for the undamaged material
- Damage initiation predicted using the quadratic nominal stress criterion
- Linear degradation law function of the dissipated energy
- The Benzeggagh-Kenane [20] (BK) law for the mixed opening mode
- The interfacial material properties are matrix dominated. For this reason the following assumptions were made:
    - Normal modulus $K_{nn}=E_2$
    - Normal strength $t_n=Y_t$
    - Equal shear moduli in both directions $K_{ss}=K_{tt}=G_{12}$
    - Equal shear strengths in both directions $t_s=t_t=S_{12}$

The parameters K_{nn}, K_{ss}, K_{tt}, t_n, t_s and t_t are defining strength, stiffness and fracture energy of the CZM model, as described in detail in the ABAQUS manual [21]. In the approach chosen here, these parameters are defined by the readily available ply properties from Table 1.

3.3. Numerical implementation

The impact and the subsequent CAI tests were numerically simulated using the finite element software Abaqus Explicit 6.14 [22].

In order to use the damage model reported in the previous sections, each composite layer (both composite layers and cohesive interfaces) needed to be modelled separately. Two C3D8R elements were used through the thickness in each composite ply. This element is the standard continuum solid hexahedral element with eight nodes and the reduced integration scheme [22]. The intralaminar damage model, implemented by means of a VUMAT subroutine [23], was integrated in the elements and evaluated for each integration point at each time increment. The hourglass, by means of the enhanced method, and the distortion controls were used for all of the elements [22].

The interfaces between the differently oriented composite plies were discretized using the cohesive element COH3D8 [22] using the classical bilinear traction separation law. Each of the interfaces was modelled with a finite thickness of 0.1 mm, which was deducted from the thickness of the adjacent layers to obtain the same total laminate thickness. The total cohesive thickness, compared to the global thickness, represented 2.9% for laminate L1, 5.8% for laminate L2 and 8.7% for laminate L3. The cohesive thickness of 0.1 mm was chosen after several trials to obtain the best compromise between the computational time and the reduction of the global laminate stiffness related to the presence of the cohesive interface [24].

All three laminates were discretized with a very fine mesh; cohesive elements of 0.5 x 0.5 mm^2 (one element in the thickness direction) and solid elements of 1 x 1 mm^2 (two elements in the thickness direction for each ply). A constant in plane ratio of one to four was used between the solid and cohesive elements as suggested in [24]. The composite and cohesive layers were coupled together by tie constrains. This method is quite complex but it gives the possibility to obtain a better control of the element sizes between the cohesive and composite layers. A finer mesh was used in the cohesive layers without leading to the same increase in the remaining elements of the laminate, optimizing the total required computational time.

The progressive damage development during the simulation can induce a localized reduction of element stiffness. This can induce excessive distortions of both brick and cohesive elements, with possible consequence of numerical instability. To reduce these problems, the fully damaged elements were excluded from the calculation.

The impact and CAI tests were simulated as three sub sequential steps within the same dynamic simulation:

1. *Impact:* simulation of the impact event and evaluation of the induced damage on the sample
2. *Stabilization:* Viscous pressure was applied on the sample to supress any residual vibration after the impact
3. *CAI:* simulation of the compression phase (including change of the boundary conditions) until failure

Through this approach, the CAI test was simulated using a dynamic solver, Abaqus Explicit, instead of the more classical implicit resolution method required for quasi-static condition (for CAI the displacement application rate is 0.5mm/min). This approach was chose mainly to remove the necessity of implementing complex tools to convert the damaged model generated by the explicit impact simulations to the implicit solver. Even more, the use of explicit solver eliminated the convergence issues of implicit methods when large geometrical and material non-linarites behaviour occurs (as the damage evolution during the CAI). In the following each step is described.

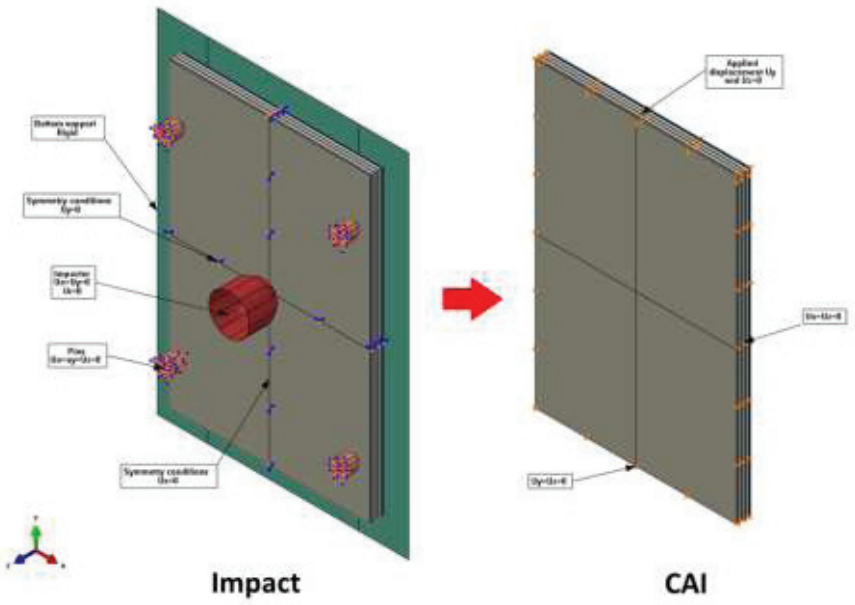

Figure 2: Impact and CAI boundary conditions and modelling approach

Step 1: Impact Simulation

For the impact simulation, the plate support was modelled as completely rigid and placed directly in contact with the samples. The four rubber pins holding the sample in place were modelled as a deformable body with a spring load of 250N on each pin. They were placed directly in contact with the upper part of the sample. The impactor was

modelled as a rigid shell body with a lumped mass of 5.02 kg (representative of the impactor mass during the test). An initial vertical velocity, according to the test set-up, was prescribed to the impactor. A force of 49 N in the vertical direction was applied to the impactor centre of mass to simulate the gravitational force (5.02 kg x 9.8 m/s^2 = 49.2 N).

The boundary conditions are schematically shown in Figure 2; they should represent the experimental conditions reasonably well [4]. In addition to the physical conditions, symmetry constraints were applied on the sample centrelines to obtain a more consistent damage development.

Step 2: Stabilization step

When the impact simulation was completed, high dynamic vibrations were still present in the model due to the reduced simulation time. An intermediate step was then included in the simulation in order to stabilize the sample before the application of the compressive for the CAI test. Viscous pressure forces were applied on both faces of the sample until the measured kinetic energy reached a value close to zero. The pressure force was calculated according to the suggestion reported in [22].

Step 3: Compression after impact simulation

After the impact and the damping steps, the CAI simulation was carried out. All the fixture and supports related to the impact test were excluded from the simulation and new boundary conditions were applied to the samples (more details in Figure 2). During the experimental test, the sample was constrained in a special fixture that restrains any out of plane movement of the sample. This was simulated by constraining the out of plane displacement of the lateral face of the sample. The compressive displacement was applied to the top edge of the sample. A constant displacement rate of 10m/min (experimental displacement applied at 0.5mm/min) was used to reduce the total computational time. As required for this type of simulations [22], it was verified that, for the selected displacement rate, the kinetic energy of the system was lower than 1% of the total internal energy of the model.

Mass Scaling: All the simulations were carried out without mass scaling to prevent any effect on the accuracy of the results. This decision is in contrast to what other authors have done in the past for similar type of simulations [4, 25, 26], but due to the model dimension and the available computational power, there was no reason to use the mass scaling with the consequent possibility of affecting the results.

Contact: The contacts between the impactor, the specimen, the support and the pins were simulated by the use of the general contact algorithm with a penalty enforcement method [27]. Moreover, due to the possible deletion of the cohesive element by reaching full damage, the same contact formulation was also applied between all the composite/cohesive layers to prevent any unnatural penetration. The Coulomb model was selected for the friction formulation for all the used contacts. The friction coefficient is strictly related to the material in contact and the surface quality. No experimental data were measured for the material used here. Several studies are available in literature [28, 29] that investigated the friction between the delaminated surfaces showing variation of friction due to the interface angle. Reported friction coefficients are in the range between 0.2 for a $0^0/0^0$ interface and 0.8 for a $90^0/90^0$ interface for GFRP. In the current work, an average friction coefficient, μ=0.3, was used for all of the implemented contacts with no variation for the different interfaces.

Simulation time and computational cost: An average of 640 K elements was obtained for the different models. The FE simulations were computationally expensive; approximately 40 GB of memory was needed with a total computational time of about 50 to 100 h (depending on the layup) on two cluster nodes with a total of 32 cores at 2.60 GHz. The long computational time is directly related to the very small stable increment time required for this type of simulation. A consistent reduction of the computational time could have been obtained using selective mass scaling.

4. Numerical/experimental comparison

The numerical impact and CAI curves are compared with the averaged experimental data in Figure 3. The numerical simulation showed in general a very good agreement with the experimental data both for the impact event and the subsequent compression test.

The maximum compressive force was accurately predicted for the different tested configurations (both for the layup variation and the incident energy). The model was capable to predict the increased damage, both inter/intra laminar, induced by higher impact energy and the consequent reduction of the capable compressive strength.

The influence of ply clustering, with the consequent variation of the impact induced delamination shape and size was correctly predicted by the numerical model. The variation in the residual compressive strength was correctly evaluated.

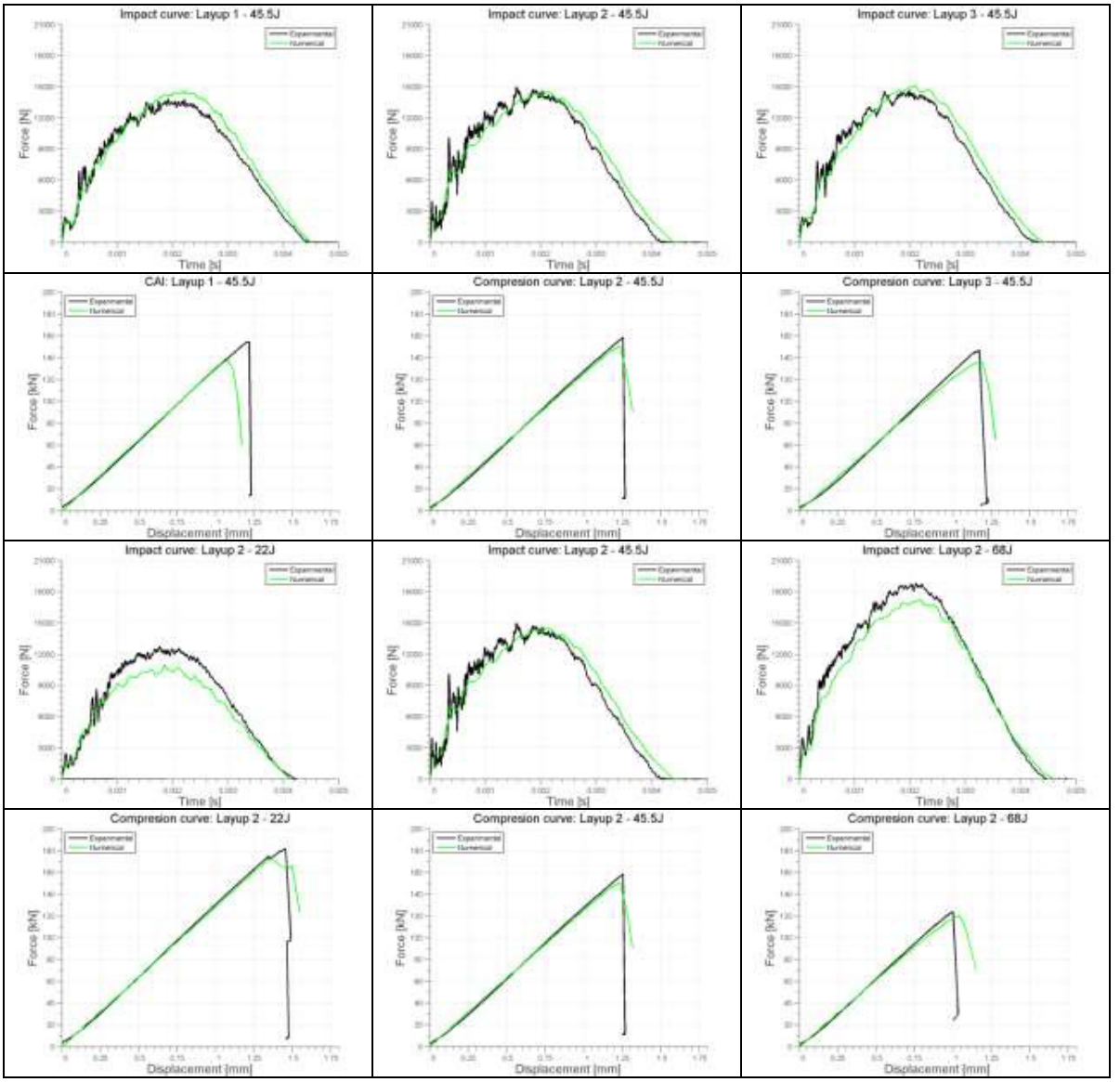

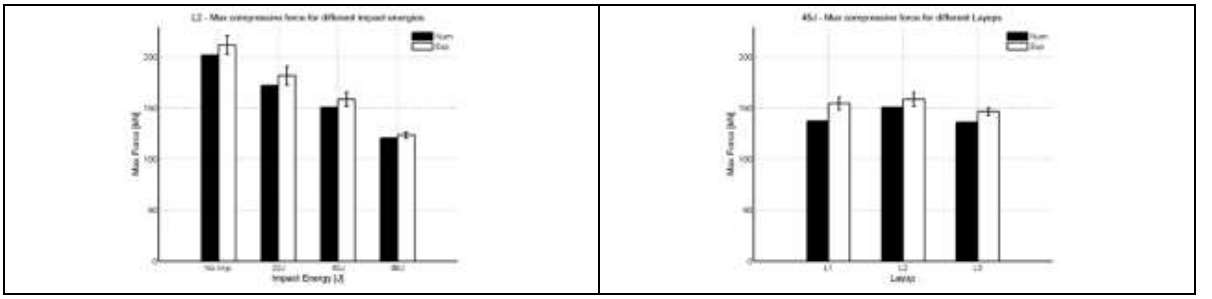

Figure 3: Impact and CAI boundary conditions and modelling approach

5. Conclusion

Experimental impact and compression after impact tests were conducted on flat cross-plied composite laminates produced with E-Glass fibres and epoxy by vacuum infusion. The experimental impact curves were compared with numerical simulations to evaluate the accuracy of the finite element model here presented.

The results clearly show that the numerical model using only simple and typically available measured material data was able to predict the impact behavior and residual material strength for the different energies and stacking sequences. A powerful and simple tool to analyze the impact behavior of thick E-Glass fiber composite using the classical in plane material properties was presented and verified against experimental tests.

References

[1] S. Abrate, Impact on composite structures., Cambridge University Press1998.
[2] L.S. Sutherland, C. Guedes Soares, Impact behaviour of typical marine composite laminates, Composites Part B: Engineering 37(2–3) (2005) 89-100.
[3] S. Abrate, J.F. Ferrero, P. Navarro, Cohesive zone models and impact damage predictions for composite structures, Meccanica 50(10) (2015) 2587-2620.
[4] E.V. González, P. Maimí, P.P. Camanho, A. Turon, J.A. Mayugo, Simulation of drop-weight impact and compression after impact tests on composite laminates, Composite Structures 94(11) (2012) 3364-3378.
[5] A. Turon, P.P. Camanho, J. Costa, C.G. Dávila, A damage model for the simulation of delamination in advanced composites under variable-mode loading, Mechanics of Materials 38(11) (2006) 1072-1089.
[6] P. Maimí, P.P. Camanho, J.A. Mayugo, C.G. Dávila, A continuum damage model for composite laminates: Part I – Constitutive model, Mechanics of Materials 39(10) (2007) 897-908.
[7] P. Maimí, P.P. Camanho, J.A. Mayugo, C.G. Dávila, A continuum damage model for composite laminates: Part II – Computational implementation and validation, Mechanics of Materials 39(10) (2007) 909-919.
[8] S.T.D. Pinho, C. G.; Camanho, P. P.; Iannucci, L.; Robinson, P., Failure Models and Criteria for FRP Under In-Plane or Three-Dimensional Stress States Including Shear Non-Linearity, NASA Technical reports NASA/TM-2005-213530, L-19089 (2005).
[9] C. Bouvet, B. Castanié, M. Bizeul, J.-J. Barrau, Low velocity impact modelling in laminate composite panels with discrete interface elements, International Journal of Solids and Structures 46(14–15) (2009) 2809-2821.
[10] S. Rivallant, C. Bouvet, N. Hongkarnjanakul, Failure analysis of CFRP laminates subjected to compression after impact: FE simulation using discrete interface elements, Composites Part A: Applied Science and Manufacturing 55 (2013) 83-93.
[11] A. Puck, J. Kopp, M. Knops, Guidelines for the determination of the parameters in Puck's action plane strength criterion, Composites Science and Technology 62(3) (2001) 371-378.
[12] A. Puck, H. Schürmann, Failure analysis of FRP laminates by means of physically based phenomenological models, Composites Science and Technology 62(12-13) (2001) 1633-1662.
[13] Hashin, Failure criteria for unidirectional composites, J Appl Mech 47 (1980) 329-34.
[14] G. Perillo, S. Shchebetov, A.T. Echtermeyer, Static ply properties: HiPer-tex™/Epoxy composite, Composites and Polymers Report Series, NTNU - Department of Engineering Design and Materials, Trondheim, 2012, p. 12.
[15] ASTM D7136 / D7136M: Standard Test Method for Measuring the Damage Resistance of a Fiber-Reinforced Polymer Matrix Composite to a Drop-Weight Impact Event.
[16] ASTM D7137 / D7137M: Standard Test Method for Compressive Residual Strength Properties of Damaged Polymer Matrix Composite Plates.
[17] G. Perillo, N.P. Vedvik, A. Echtermeyer, Numerical analyses of low velocity impacts on composite. Advanced modelling techniques., Proceedings of the Simulia Customer Conference - 2012 (2012).
[18] G. Perillo, N. Vedivik, A. Echtermeyer, Damage development in stitch bonded GFRP composite plates under low velocity impact: Experimental and numerical results, Journal of Composite Materials (2014).

[19] G. Perillo, N.P. Vedvik, A. Echtermeyer, Numerical and experimental investigation of impact on filament wound glass reinforced epoxy pipe, Journal of Composite Materials (2014) 16.
[20] M.L. Benzeggagh, and M. Kenane, Measurement of Mixed-Mode Delamination Fracture Toughness of Unidirectional Glass/Epoxy Composites with Mixed-Mode Bending Apparatus, Composites Science and Technology 56 (1996) 439–449.
[21] I. Abaqus, Abaqus Version 6.14 User's manual, (2014).
[22] Abaqus 6.14: Analysis User's Manual.
[23] Abaqus 6.14: User Subroutines Reference Manual.
[24] A. Turon, C.G. Dávila, P.P. Camanho, J. Costa, An engineering solution for mesh size effects in the simulation of delamination using cohesive zone models, Engineering Fracture Mechanics 74(10) (2007) 1665-1682.
[25] C.S. Lopes, P.P. Camanho, Z. Gürdal, P. Maimí, E.V. González, Low-velocity impact damage on dispersed stacking sequence laminates. Part II: Numerical simulations, Composites Science and Technology 69(7–8) (2009) 937-947.
[26] W. Tan, B.G. Falzon, L.N.S. Chiu, M. Price, Predicting low velocity impact damage and Compression-After-Impact (CAI) behaviour of composite laminates, Composites Part A: Applied Science and Manufacturing 71 (2015) 212-226.
[27] I. Abaqus, Abaqus 6.11 User's Manual, (2011).
[28] J.K. Lancaster, The effect of carbon fibre reinforcement on the friction and wear of polymers, Journal of Physics D: Applied Physics 1(5) (1968).
[29] J. Schön, Coefficient of friction of composite delamination surfaces, Wear 237(1) (2000) 77-89.